SPATIAL AND TEMPORAL PRECIPITATION AND THEIR EFFECTS ON QUEETS WATERSHED RUNOFF IN THE OLYMPIC EXPERIMENTAL STATE FOREST

By

TRAVIS E. LOPES

A thesis submitted in partial fulfillment of

the requirements for the degree of

MASTER OF SCIENCE IN CIVIL ENGINEERING

WASHINGTON STATE UNIVERSITY

Department of Civil and Environmental Engineering

AUGUST 2010

To the Faculty of Washington State University:

The members of the Committee appointed to examine the thesis of TRAVIS E. LOPES find it satisfactory and recommend that it be accepted.

_____

Michael Barber

_____

Jennifer Adam

_____

Balasingam Muhunthan

ACKNOWLEDGEMENTS

I would like to begin by mentioning by advisor and committee chair, Dr. Michael Barber, and express my sincere gratitude for his help and guidance. His knowledge and support were well needed for the completion of this project. I would also like to thank the other members of my thesis committee, Dr. Jennifer Adam and Dr. Balasingam Muhunthan, for their constructive criticism and help with ideas and guidance. My sincerest appreciation is held for Muhammad Barik and his help with setting up DHSVM and providing me with much of the needed data used. Lastly I would like to offer my thanks to my parents, family, and friends for their support and patience throughout this process.

SPATIAL AND TEMPORAL PRECIPITATION AND THEIR EFFECTS ON QUEETS WATERSHED RUNOFF IN THE OLYMPIC EXPERIMENTAL STATE FOREST

Abstract

by Travis E. Lopes, M.S.
Washington State University
August 2010

Chair: Michael E. Barber

Hydrologic characteristics of the mountainous Olympic Peninsula in western Washington State are unique due to the regions' proximity to the Pacific Ocean. Abundant moisture and steep terrain result in significant orographic precipitation that produces challenging land management decisions regarding timber harvesting activities in the Olympic Experimental State Forest (OESF) especially when factoring climate change into future runoff predictions. Two important issues are examined in this paper. First, the spatial extrapolation of topographic precipitation variation from sparse weather data is examined by evaluating PRISM adjusted precipitation in the OESF using a dynamic hydrology model called DHSVM. Second, while it is projected that increases in future monthly precipitation for the Olympic Peninsula are likely, little is understood about how the actual timing of these precipitation increases will impact future runoff and thus precipitation projections overall are highly uncertain. Using the DHSVM model, variations in temporal rainfall patterns under 3 different GCM projections for 2 climate

scenarios representing 2050 climate change predictions were examined. It was determined that precipitation may be underestimated by as much as 61%. However, DHSVM runoff results do not compare with this underestimation with an under prediction of approximately only 9% for the 2006 water year. In addition it has been shown that accurate daily time scale increments of precipitation are needed in order to predict the magnitude of peak runoff events and total annual runoff under different climate change scenarios. It was found that average annual flow could vary by more than 23% from the current average flow for the Queets basin across different time scales. In addition, it was determined that peak runoff events could vary by more than 40,000 ft^3/s (1,133 m^3/s) in magnitude. These results demonstrate the need for accurate spatial interpolation and reliable down scaling techniques used for future precipitation projections when attempting to predict landslides.

TABLE OF CONTENTS

Page

ACKNOWLEDGEMENTS iii

ABSTRACT iv

LIST OF TABLES vii

LIST OF FIGURES viii

1.0 INTRODUCTION 1

1.1 REGION OF INTEREST 7

1.2 PRISM 8

1.3 DHSVM 12

1.4 METEOROLOGICAL DATA 13

2.0 METHODS 13

2.1 ANALYZING PRISM AND METEOROLOGICAL DATA 13

2.2 TEMPORAL EFFECTS 16

3.0 RESULTS 20

3.1 PRISM AND METEOROLOGICAL DATA EVALUATION 20

3.2 TEMPORAL EFFECTS 24

4.0 CONCLUSION 32

REFERENCES 36

LIST OF TABLES

1. Rainfall Events 18

2. Calculated Runoff Coefficients 24

LIST OF FIGURES

1. PRISM conceptual framework 11
2. GIS Clip of PRISM Data 15
3. GCM Projected Precipitation Changes 19
4. Seasonal GCM Precipitation Changes 20
5. Discharge Results for Unmodified Precipitation Data 23
6. Annual Runoff Percent Difference from Unadjusted 27
7. Annual Runoff Results 28
8. Time Series Plots 30
9. Residual Plots, 3 hour vs. Monthly 31

1.0 INTRODUCTION

Spatial and temporal variability in precipitation directly influence surface runoff and groundwater infiltration in watersheds (Bloschl and Sivapalan, 1995). When predicting catchment hydrology with physically-based models, it is critically important to correctly characterize the amount, location, and timing of precipitation since accurate representation of incoming water is essential for model process calibration and validation. Furthermore, this ultimately allows for accurate and objective analyses of model results under future land use conditions (Beven and Binley, 1992; Serreze et al. 1999 ; Zhang and Srinivasan 2009). Calibration of dynamic hydrologic models is often carried out using historical meteorological data and changing the parameters governing evapotranspiration, infiltration, and runoff processes based on comparison of modeled stream flow results to observed historical stream flow data (Jakeman and Hornberger, 1993). When model results are found to diverge from the observed stream flow data it is typically prudent to examine the meteorological data for errors after which reasonable adjustments are made to model parameters in an attempt to account for the discontinuities between the predicted and observed stream flow data. However, it is often difficult to validate meteorological data where there is little observational data thus potentially leading to a misrepresentation of model parameters. For example, models that under estimate the spatial distribution of precipitation must corresponding compensate in the calibration phase by reducing evapotranspiration and/or infiltration in order to match predicted and measured stream discharges. This can further lead to erroneous predictions of land use change scenarios and hazard analyses involving landslides or flooding.

Motivation for a better understanding of spatial and temporal variations in precipitation in the Olympic Experimental State Forest (OESF) arises from the connection between precipitation, forest management, and landslide events. Landslides in this area are a threat to human life and can cause significant environmental damage to salmonid habitat. Storck et al. (1998) and Moore and Wondzell (2005) identified the linkages between timber harvesting and runoff processes in Pacific Northwest forests. Guzzetti et al. (2008) observed that one of the primary causes of shallow landslides was high intensity and/or long duration rainfall. It has also been shown that rainfall percolation into the soil leads to a reduction in shear strength and is a primary trigger of shallow landslides (Terlien 1998). This is a result of increased groundwater infiltration that leads to increased pore water pressure and decreased slope stability (Iverson 2000). Any uncertainty in the processes driving water percolation into the soil can cause a misrepresentation of the susceptibility of a slope to failure. This lends credence to the importantance of correctly representing the spatial precipitation in order to correctly represent model parameters contributing to slope stability.

Observations of precipitation are gathered through rain gauge networks located around the world. However, due to rain gauge location and the exiguousness of rain gauge networks, methods for interpolating the observations spatially are often employed in order to estimate precipitation anywhere within an area of interest.

Methods of creating gridded precipitation data sets range from simple to complex, but overall fall into three categories (physical, statistical, or remote sensing). Physical approaches were the earliest methods used and include the Thiessen Polygon

method (Thiessen 1911) and isohyetal plots interpolated using elevation data (Peck and Brown 1962). As the interactions between topography and precipitation have become better understood and computing power has increased, more statistical approaches have been used. Houghton (1979) used multiple regressions of various topographic parameters such as slope, aspect, elevation, and location correlated with point precipitation data to estimate spatial precipitation in the Great Basin region west of the Sierra-Nevada Mountain Range. Similar approaches using GIS-based technology with regression or multiple kriging approaches have been proposed (Marquínez et al., 2003; Guan et al., 2005; Zhang and Srinivasan 2009). Kadiglu and Sen (1995) developed power-law expressions for distributing monthly of wet and dry periods in Turkey. A standardized point cumulative semivariogram (SPCSV) methodology was used by Sen and Habib (2000) for identification of a precipitation-elevation relationship. Likewise Brown and Comrie (2002) proposed a statistical modeling technique for a topographically varying domain capable of yielding mean and interannual gridded climate datasets. Remote sensing techniques have also been used to create gridded precipitation data sets. Most notably are the methods used in the Next Generation Weather Radar (NEXRAD) system that formulates precipitation estimates based on measured radar reflectivity values (Hultstrand et al., 2008). Satellite remote sensing techniques also are attempting to measure the infrared emissivity of cloud tops, using developed algorithms to relate the temperature of the cloud tops to surface precipitation (Kidd et al., 2003).

In addition to the processes described above, two models have been developed that employ local regression techniques to interpolate precipitation observations. In an

effort to establish a nationally consistent approach, the Precipitation Regression on Independent Slopes Model (PRISM) has been used to make gridded precipitation estimates at approximately a 4 km scale based from point precipitation data and topographic characteristics (Daly et al., 2002). A similar approach for predicting temperature, precipitation, humidity, and radiation called Daymet was developed at the University of Montana. The methods used to create the Daymet data set include a truncated Gaussian weighting filter for interpolation, and local linear regressions of precipitation versus elevation (Thornton et al., 1997). 500 m Digital Elevation Model data obtained from the United States Geological Survey (USGS) and meteorological observation data gathered from the National Climatic Data Center (NCDC) National Weather Service (NWS) were used to make 1 km gridded meteorological data (Thornton et al., 1997). While Zimmermann and Roberts (2001) concluded DAYMET offers superior theoretical procedures for temperature downscaling, PRISM is still widely used in the United States. The meteorological data used (discussed in section 1.4) and PRISM were evaluated in this study in an attempt to observe possible under or overestimation errors as related to their precipitation estimates for the study region.

Uncertainties in precipitation estimates can be compounded when temporal effects are considered. Temporal trends in precipitation resulting from either natural climate variations or those expected to occur from global climate change both result in hydrologic variability over time. Land management decisions that incorporate climate change induced precipitation changes are required to protect humans and ecosystems from mass wasting events. Xu and Halldin (1997) found that a 20% change in annual

precipitation increased annual runoff by 31 to 51% in their 13 high latitude catchments with annual runoff coefficients ranging from 0.32 to 0.45 (average = 0.37).

Under many global climate change model (GCM) predictions annual precipitation is expected to continue to increase in Washington (Diffenbaugh et al., 2005; Leung and Wigmosta 1999; Miles et al., 2000). However GCM projections for precipitation are highly uncertain and are highly variable across the range of different GCMs and down scaling procedures. Despite the increases in precipitation, Fu et al. (2009) demonstrated that streamflows in Washington decreased over the past 50 years partially reflecting the increases in evapotranspiration and water use. Understanding the complex interactions affecting the hydrology of a region resulting from the timing of precipitation increases is key in evaluating the magnitude of the impacts.

Several methods have been proposed to downscale GCM data to spatial and temporal scales needed for local and regional analysis, and to help with issues of uncertainty and variance of GCM precipitation projections. A simple method to account for uncertainty in GCM precipitation projections is to employ the projections for several GCMs to create an ensemble. In this case, the historical precipitation data is scaled by a delta change representing a GCM projection. The results of all the different GCM delta change applications are then presented together to give a mean and range of expected precipitation changes. However, this does not account for temporal variances in precipitation patterns, thus ignoring magnitude and frequency of storm events (Chiew et al., 2003). Stochastic weather generators have been used to create synthetic data that accommodate temporal variances by matching changes in statistical parameters such as mean and variance of the regional climate to changes at the GCM scale

(Semenov and Barrow, 1997). Stochastic downscaling offers a third approach to apply GCM projected climate changes to meteorological data. This method involves relating large atmospheric circulation parameters to the catchment scale, and is advantageous over the previously mentioned methods because of a better understanding of atmospheric circulation as compared to precipitation processes (Stehlik and Bardossy, 2002).

The goal of this study was not to evaluate the methods of temporal downscaling, but to determine how intensity and duration of projected precipitation changes affects runoff, thus provide guidance into time increment requirements in future down scaling efforts. Katz and Brown (1992) showed that changes in the variability of climate variables provided a better correlation with extreme events as opposed to changes in mean values. Additionally, it has been found that high-intensity storm events can be attributed as triggering factors for several shallow slides, whereas lower-intensity events lasting longer in duration have the ability to cause larger more complex slides (Zezere et al., 1999). When incorporating scalar percentage increases associated with GCM precipitation projections, storm intensity and duration are inversely proportional to one another. It is important to understand how varying the magnitude and duration of GCM projected precipitation changes affects runoff in order to offer correlation with storm events and runoff.

This paper describes the evaluation of using PRISM to interpolate precipitation and the effects of adjusting the timing of precipitation increases resulting from global climate change for a mountainous catchment contained in the Olympic Experimental State Forest (OESF). The Distributed Hydrology-Soil and Vegetation Model (DHSVM)

by Doten et al. (2006) was used in this study to model the catchment hydrology. Runoff coefficients have been calculated using PRISM precipitation and USGS runoff data. Resulting runoff estimates are shown for varying the intensity and duration of projected precipitation changes due to global climate change. This information will ultimately be used for improved prediction of landslides in response to land management decisions in the region.

1.1 REGION OF INTEREST

The OESF is located on the Olympic Peninsula in Washington State abutting the Pacific Ocean. The OESF consists of 264,000 acres (107,000 ha) of state trust land dedicated for experimentation of forestry techniques with a primary goal of integrating timber production and habitat conservation (Policy for Sustainable Forests, 2006). The temporal and spatial distribution of precipitation is extremely variable with average annual precipitation ranging from 15.7 to 138 inches (400 mm to 3500 mm); the majority of which falls between the months of October and March (Polluck et al., 2004). Elevation in the OESF is also highly variable ranging from sea level to approximately 8000 ft (2400 m) on peaks in the Olympic Mountains. Precipitation has been shown to increase by 50 to 70% from valleys to adjacent ridge-tops in the western Olympic Mountains (Minder et al., 2008). In addition, rainfall has been shown to vary by an order of magnitude between the windward and leeward facing slopes in the Olympic Mountains (Colle et al., 1999). This study focuses on the Queets basin, a 449 mi^2 (1,163 km^2) watershed in the OESF with an average annual flow of approximately 4,300 ft^3/s (121 m^3/s).

1.2 PRISM

Mountainous terrain can cause significant underestimation errors in extrapolated rain gauge data. This can be a result of rain gauge locations (typically in low-lands and valleys) since precipitation generally increases with elevation (Smith, 1979). Daly et al. (2002) has proposed one method to accommodate mapping precipitation in areas of rough terrain and difficult climate conditions called PRISM. PRISM provides a method to spatially distribute point measurements (rain gauge data) to a gridded cell network at regional to continental scales (Daly et al., 1994). Through the use of linear regressions, extracted from rain gauge data and elevations, this model extrapolates known precipitation data to mountainous topography. Figure 1 shows the conceptual framework under which PRISM operates.

On the PRISM website (http://www.ocs.orst.edu/prism/) data sets are available for mean monthly and annual precipitation, maximum, minimum, and average temperature, dew point temperature, relative humidity, snowfall, heating and cooling days, and growing degree days, median last spring freeze and first fall freeze dates, median freeze-free season length, and others for 1961-1990 (Daly et al., 2000).

A fundamental concept used in the PRISM framework is the idea of assigning similar slope aspects, called a “facet” an identification tag. Facets are determined from a DEM of the area of interest. An unfiltered, 5-minute DEM is used to extract one facet grid, and then 8, 16, 24, 32, and up to 40 filtering passes are applied to this same DEM to accommodate rain gauge networks where data is limited (Daly et al., 1994). This methodology may pose a problem when applied to the OESF because sparse rain

gauge data and rapidly changing topography may cause PRISM to filter out many of the important topographic features of the OESF. In an effort to eliminate this concern, PRISM assigns a set linear precipitation regression based on the mean all available regression slopes analyzed but in the range of 0.38 to 0.82 in/mi (0.6 to 1.3 cm/km) along slopes that are too steep to be seen in the course resolution DEM (Daly et al., 1994). Another fundamental issue that may be a problem is that the model assimilates facets that straddle mountain crests into adjacent facets (Daly et al., 1994). This could pose a problem because the Olympic Mountains are characterized by heavy precipitation, with more than 9.8 ft (3 m) per year in the Hoh River Valley on the windward southwest facing slopes and an intense rain shadow (only 1.3 ft (0.4 m) of annual precipitation in Sequim) on the leeward northeast facing slopes (Anders et al., 2006). PRISM could under or over estimate precipitation values by incorporating facets into adjacent facets in areas where they straddle southwest/northeast mountain ridges. In a last attempt to buffer discontinuities caused by topography in the model produced gridded precipitation regressions, PRISM uses a postprocessor called Gradient to ensure that all regression slope values are less than the maximum slope allowable or 1.9 in/mi (3.0 cm/km).

One aspect lacking from the PRISM framework is gauge undercatch and bias adjustments. Bias is introduced into rain gauge observations through several mechanisms including undercatch of precipitation due to wind deformation above the gauge, losses induced from water adhering to the gauge surface, evaporation from the gauge, raindrop splash, blowing snow, trace precipitation being treated as zero, and gauge recording techniques (Adam and Lettenmaier, 2003). Snow dominated regions

are more affected by gauge undercatch because of the amount of precipitation falling in solid form. Snow, as opposed to liquid precipitation, is more able to be blown into or out of the gauge and is more affected by the wind field deformation above the gauge. Yang and Ohata (2001) determined that precipitation was represented by as little as 50% by the gauge observations in Siberia, and Adam and Lettenmaier (2003) found a 11.7% annual increase in global precipitation upon applying gauge undercatch and bias adjustment techniques to rain gauges worldwide.

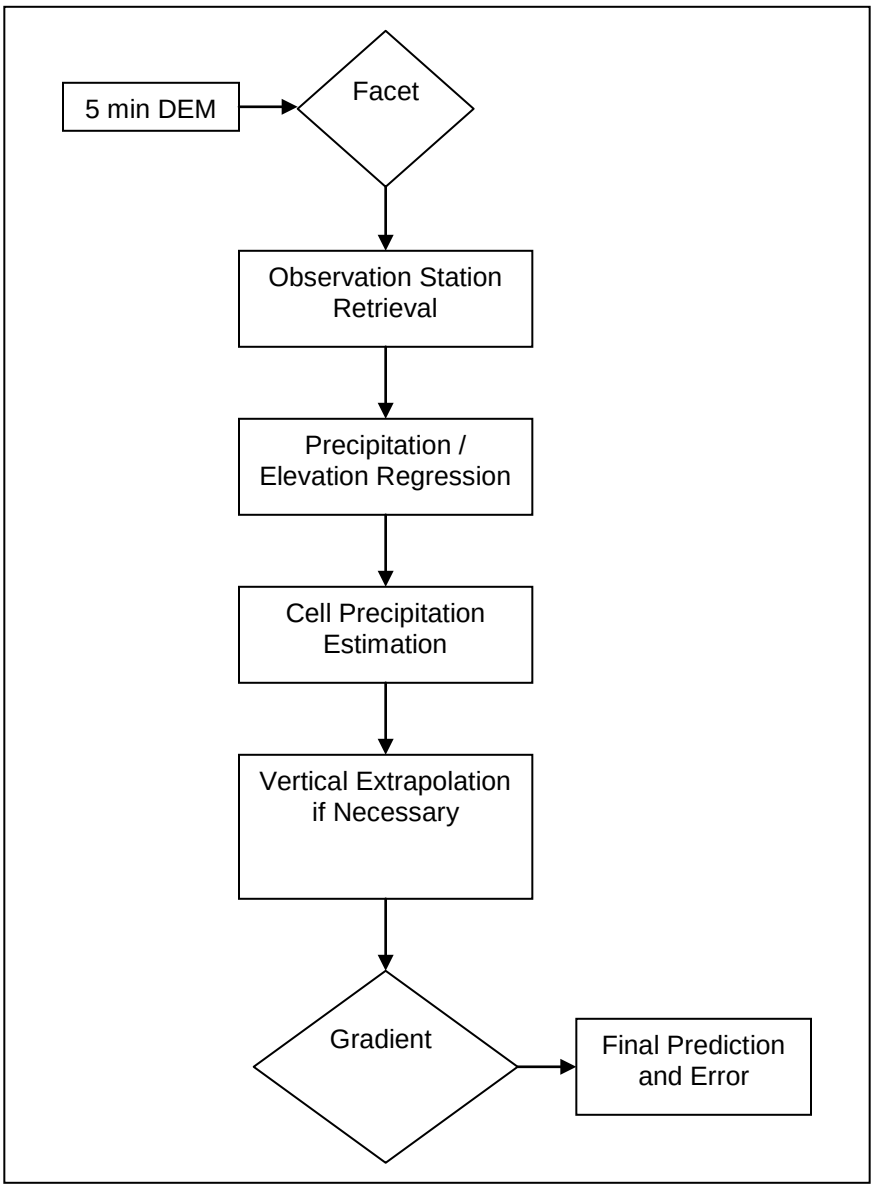

Figure 1 – PRISM conceptual framework.

1.3 DHSVM

The Distributed Hydrology Soil Vegetation Model (DHSVM) version 2.0 enables the determination of relationships between precipitation and runoff by dynamically simulating basin characteristics such as soil moisture and outflow based from 30 m to 200 m resolution digital elevation model (DEM) and climate data (Wiley and Palmer 2008). The model is comprised of seven modules including evapotranspiration, snowpack accumulation and melt, canopy snow interception and release, unsaturated moisture movement, saturated subsurface flow, surface overland flow, and channel flow that combined simulate a coupled water (mass) and energy balance (Wigmosta et al. 2002). DHSVM is run on a Linux platform and requires inputs of DEM data, soil type, vegetation map, and meteorological forcings. A basin mask is also required to limit the areal extent of the model simulations to the area defined by the user. Wigmosta et al. (2002) gives a detailed description of the model processes.

Several studies have been conducted evaluating DHSVM and the applications of the model (Nijssen et al., 2007; Lamarche and Lettenmaier, 1998; Bowling and Lettenmaier, 2001; and Wigmosta and Perkins, 2001). The model has also been used in applications concerning forest management (Storck et al., 1995; Lamarche et al., 1998; Bowling et al., 2000; Wigmosta and Perkins, 2001). Storck et al. (1995) used DHSVM to study the effects of forest harvesting on floods for the Snoqualmie River at Carnation finding a statistically significant increase in smaller floods (flows less than 23,000 ft^3/s (650 m^3/s)) for a 46-year period (1948-1993). DHSVM has also been used to study the effects of roads on evapotranspiration, soil moisture, depth to water table, and stream discharge for a catchment in Northern Thailand (Cuo et al. 2006).

1.4 METEOROLOGICAL DATA

The meteorological forcings used in this study consist of a 1/16th degree gridded data set developed by Deems and Hamlet (2010). This data set is an improved (finer spatial resolution and temperature rescaling) and extended record (1915-2006) of the data constructed by Maurer et al. (2002). The data set is based on observed daily precipitation and maximum and minimum air temperature data obtained from the National Oceanic and Atmospheric Administration (NOAA) National Weather Service (NWS) primary and Cooperative (Co-op) stations. The precipitation data was scaled to match the PRISM monthly means to account for topographic effects. Daily wind estimates were derived from NCEP/NCAR reanalysis wind speed data (Kalnay et al. 1996), and relative humidity and shortwave and longwave radiation were estimated using precipitation and temperature data according to the methods described by Maurer et al. (2002). Daily meteorological data outputs were then evenly apportioned into 3 hour time steps for use with the Variation Infiltration Capacity (VIC) model (Elsner et al., 2010) and DHSVM.

2.0 METHODS

2.1 ANALYZING PRISM AND METEOROLOGICAL DATA

The meteorological data developed by Deems and Hamlet (2010) was scaled using PRISM, so therefore PRISM is the mechanism for spatially distributing precipitation of concern for this study. Due to the high degree of topographic and climatologic variability unique to the OESF, however, evaluation of PRISM was

conducted. This was accomplished by using ArcGIS 9.3 (a GIS software package) to determine water year runoff coefficients. The runoff coefficients estimated using ArcGIS were then compared to typical runoff coefficients for a heavily forested, steep slope region.

The PRISM data, acquired from the PRISM Climate Group website (www.prism.oregonstate.edu/), was converted from raster format using ArcGIS to a shapefile format to be further manipulated in ArcMap. In addition to the PRISM data, watershed basin boundaries for given watersheds contained in the OESF were acquired from the Washington State DNR GIS portal (http://fortress.wa.gov/dnr/app1/dataweb/dmmatrix.html). Both the PRISM and watershed boundary data were then imported into ArcMap for further analysis. Using the clip tool in ArcMap, the PRISM data was truncated so only the data contained in the Queets watershed remained. Figure 2 shows the PRISM data truncated for water resource inventory area 21 (WRIA 21) on the Olympic Peninsula. The PRISM data was then exported in a table format and imported into Microsoft Excel 2007 for further analysis. Using Excel the PRISM precipitation values were multiplied by their respected grid cell area and the sum of all the grid cell precipitation volumes were used as the total precipitation volume for the PRISM data. The calculated precipitation volume was then divided by USGS stream gauge data acquired from the USGS website (http://waterdata.usgs.gov/nwis/rt) to find the runoff coefficient. This was done for all months contained in water years 1996-2006.

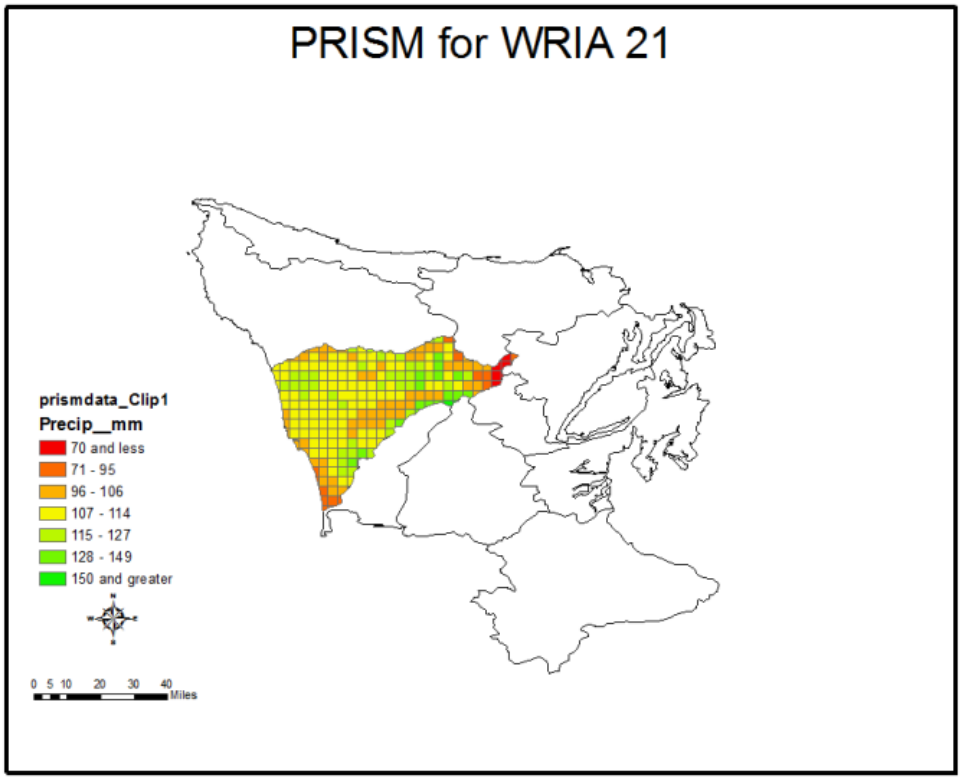

Figure 2 – GIS clip of PRISM data for WRIA 21.

Water year runoff coefficients were also determined for the meteorological data developed by Deems and Hamlet (2010) using methods similar to those discussed for the PRISM data. Using ArcGIS 9.3, only the grid cells contained within the boundaries of the Queets basin were analyzed. Precipitation volumes were determined by multiplying each grid cell precipitation depth by its representative area, and summing the result of all grid cells to arrive at a total basin precipitation volume. Grid cell areas were classified as the area inside that basin boundaries influenced by the corresponding precipitation depth. The precipitation volumes for all the grid cells were

then divided the total basin area. The runoff coefficients were determined by dividing the USGS stream gauge values by the calculated precipitation volumes.

2.2 TEMPORAL EFFECTS

Studies investigating the connection between rainfall and landslides have shown that both the critical intensity and antecedent rainfall are contributing factors in triggering landslides (Rahardjo et al., 2001; Dai and Lee 2001). Downscaling of global climate change to daily or sub-daily time increments is currently more of an art than a science. Therefore it is important to study the effects of short-duration, high-intensity storms and long-duration, low-intensity storms on runoff. In order to develop these relationships five different maximum rainfall events were established (table 1) to which GCM projected scalar percentages were applied.

To account for variability and uncertainty in GCM precipitation projections three different GCMs under two different emission scenarios (A1B and B2) were used. The A1B emission scenario delineates a storyline of rapid economic growth, a population peak mid-century then declining, introduction of new and more efficient technologies, and has a balanced emphasis across different energy sources (IPCC, 2000). The B2 storyline is characterized by less rapid introduction of technology, a constantly increasing population, and focuses on changes made at regional and local levels to offer solutions for social, economic, and environmental sustainability (IPCC, 2000). Models BCCRBCM2, CCMA-31, and GISS-ER were selected based on low, average,

and high estimates of projected precipitation for the region from twenty different GCMs (figure 3a, b).

The precipitation data was scaled temporally using a delta change method based on the seasonal projected precipitation changes (figure 4a, b) of the BCCR-BCM2.0, CCMA-31, and GISS-ER models. The projected precipitation changes were applied on a month by month basis and the total change for each month was taken as the projected scalar percentage of the entire month, or:

$$\Delta_m = \beta_s P_m \quad (1)$$

Where Δ_m is the total monthly change in precipitation, β_s is the seasonal scalar percentage change for a given month projected by the corresponding GCM, and P_m is the total monthly precipitation. Δ_m was then apportioned evenly by dividing by the number of 3 hour time intervals in the 5 different classified storm, or:

$$\alpha = \frac{\Delta_m}{(\Delta t_i/3)} \quad (2)$$

Where α is the 3 hour precipitation change and Δt is the length of the i^{th} storm event. The 3 hour precipitation change (α) was added to the meteorological data to all 3 hour precipitation estimates contained in the different lengths of storm events. The five different storm events used (table 1) consisted of 3 hour, 1 day, 2 day, 7 day, and month time increments.

Table 1 – Classified rainfall events that GCM projected precipitation changes were applied.

1	Maximum 3 hr
2	Maximum 1 day
3	Rolling maximum 2 day
4	Rolling maximum 7 day
5	Evenly over entire month

Temporal rainfall resolution effects were first analyzed under the two extreme scenarios. This first was to apply projected precipitation changes to the maximum 3 hour precipitation event for each month. The second scenario was to evenly distribute the precipitation changes to all days in a given month. The projected precipitation changes were then applied to the maximum day, 2 day, and 7 day events. The method of choosing the maximum 3 hour precipitation event focused only on the absolute maximum 3 hour precipitation interval. Due to the even apportionment of daily precipitation into three hour intervals, the maximum 3 hour event occurred during the single day maximum. The 2 day and 7 day events were classified on a rolling basis to determine the maximum event in terms of total precipitation volume. GCM projected increases were applied to all events (table 1) classified using the delta change method for the months contained in the 2006 water year to represent precipitation changes projected for 2050. The modified precipitation data were then used as meteorological inputs for DHSVM. The results from the DHSVM runs were then compared to see how

changing the temporal distribution of precipitation projections affected runoff volume and peak events in the Queets watershed.

(a)

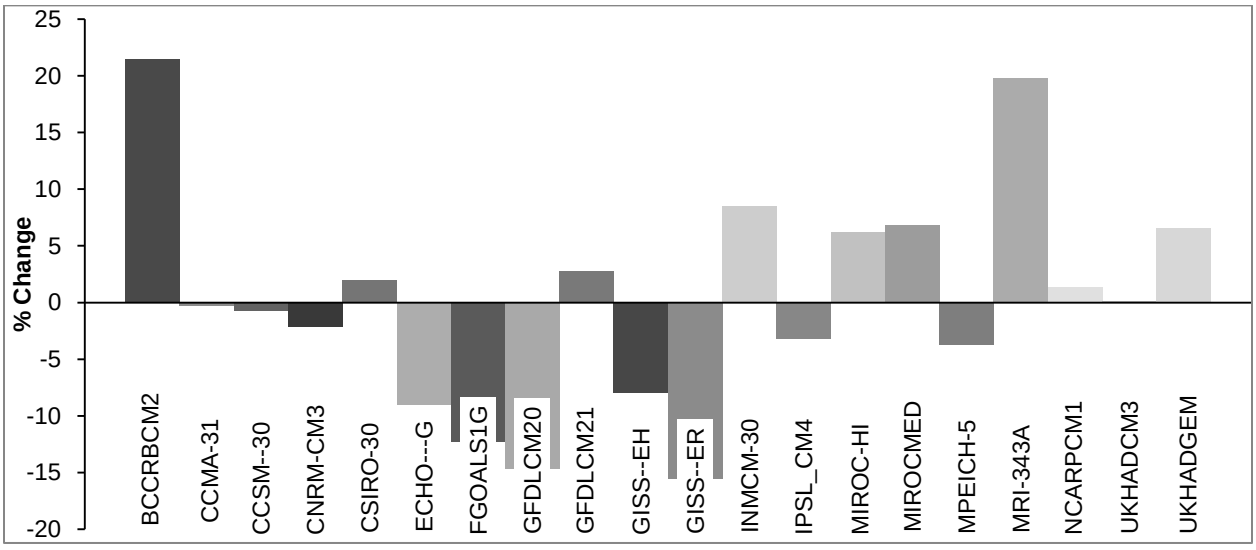

(b)

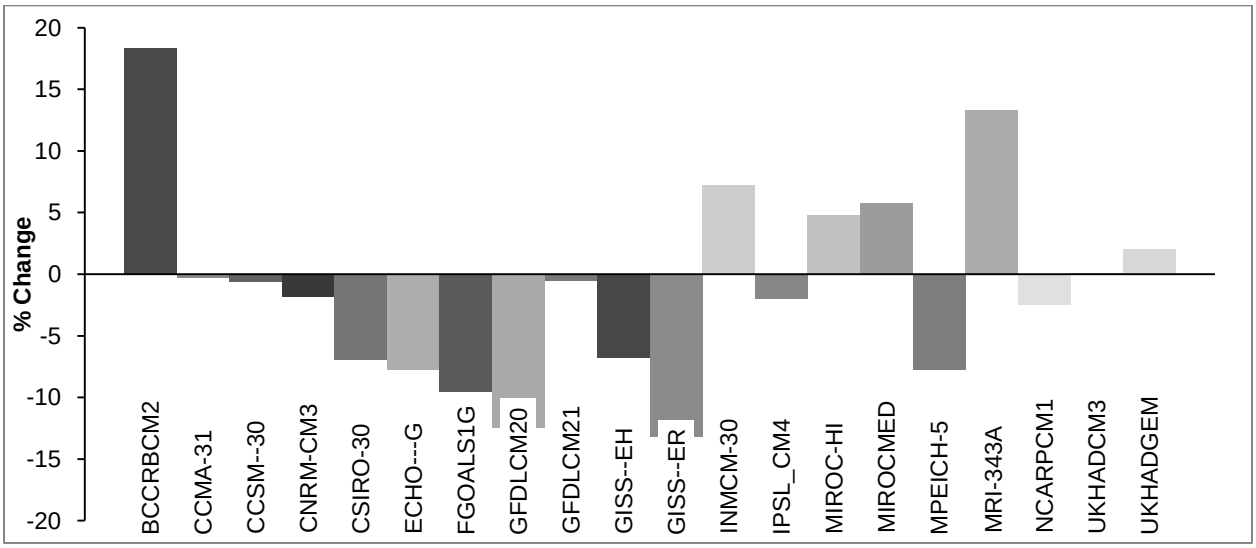

Figure 3 – Projected precipitation changes in percent from twenty different GCMs for (a) emission scenario A1B, and (b) emission scenario B2.

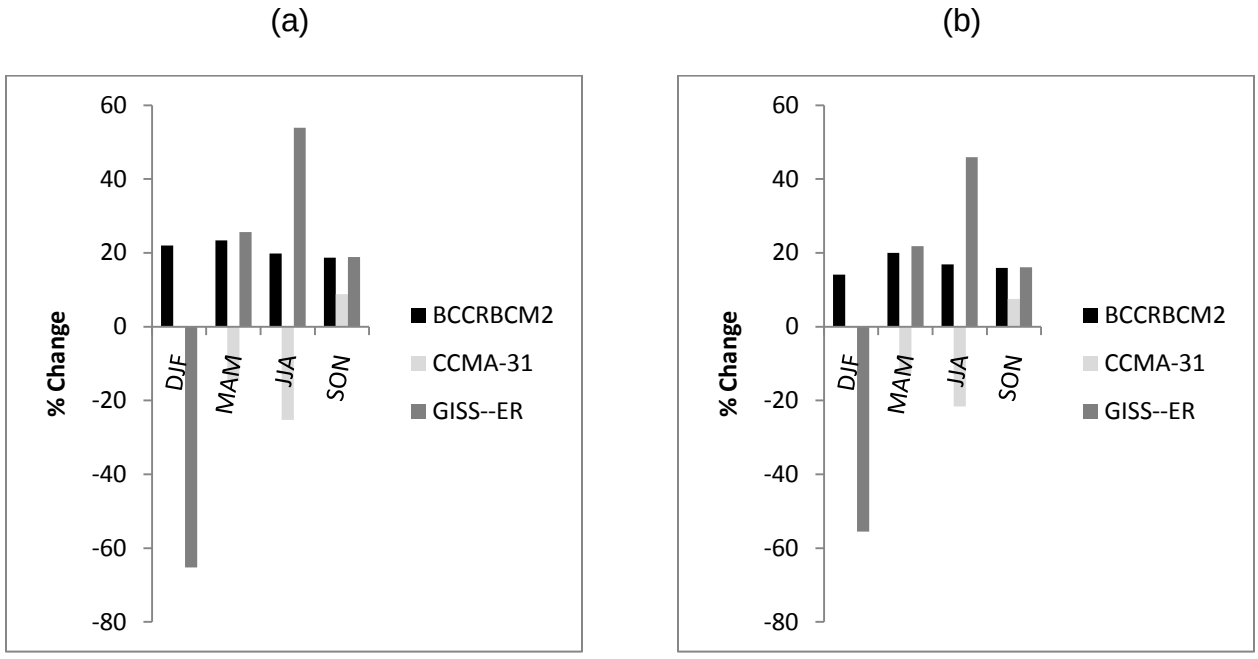

Figure 4 – Seasonal projected percentage precipitation changes of the three GCMs used in this study for emission scenario (a) A1B and (b) B2.

3.0 RESULTS

3.1 PRISM AND METEOROLOGICAL DATA EVALUATION

Using the method previously discussed to calculate runoff coefficients for the PRISM precipitation estimates resulted in a significant underestimation of total precipitation for some of the water years between 1996 and 2006. Analysis of monthly runoff versus precipitation is complicated due to the prevalence of snow at higher altitudes melting at times other than when it is actually accumulated. For this reason annual water year values represent the most consistent means of comparison. The resulting annual runoff coefficients for the 1996 to 2006 water years ranged from 0.83 to 1.13 and had an average of 0.98 (table 2). Similar results were determined for the

meteorological data (Deems and Hamlet, 2010) which had a range of 0.84 to 1.14 and an average of 0.99. Muhammad Barik, a fellow researcher at Washington State University, found an average runoff coefficient of 0.84 for the meteorological data for calendar years 1984 to 1995 and 0.85 for the PRISM data. Discrepancies in the runoff coefficient values are likely attributed to the different analysis periods.

Runoff coefficients have been found to be a function of topography, land cover, and rainfall intensity thus varying depending on site characteristics (Chow et al., 1988). Katimon and Wahab (2003) found relatively large variations in annual runoff coefficients ranging from 0.32 to 0.92 over a 13 year period with an average value of 0.61 for a peat dominated catchment in Malaysia. These values are considerably higher than urban values of annual storm runoff coefficients found in several previous studies (Heany et al., 1976; Schueler 1987; Pandit and Gopalakrishman 1996). Runoff coefficients of 0.16, 0.24, and 0.27 have been determined for catchments in the Amazon Region of French Guyana that receive as much as 4,000 mm of precipitation annually and contain slopes of up to 50% (Roche, 1981). Boorman et al. (1995) classified 29 different soil types in the UK according to their hydrologic characteristics finding runoff coefficients ranging from 0.15 to 0.60. In addition runoff coefficients have been shown to range from 0.60 in vegetated urban areas to 0.75 in urban areas that are less vegetated (Pauleit et al., 2005). Although the characteristics influencing runoff in the OESF are unique it is not unreasonable to assume a range of 0.6 to 0.9 for the runoff coefficient. Upon comparison of this range with the determined PRISM and meteorological data (Deems and Hamlet, 2010) averages, it can be shown that precipitation underestimation could be as high as 65%. However, assigning actual underestimation values is

complicated because of a lack of data concerning the true hydrology of the Queets basin.

Running DHSVM using the precipitation data unadjusted for the PRISM underestimation yielded a total annual runoff volume of nearly 9% less than the USGS recorded volume for the 2006 water year. To come even this close to the annual runoff likely means that calibration parameters under predict evapotranspiration and infiltration. Without accurate representation of these two phenomenons, future predictions of the impacts of timber harvesting will be highly suspect. Runoff events compared well temporally with observed USGS stream gauge data (figure 4). The largest underestimation occurred during low flow situations and overestimation occurred for some of the peak runoff events. Thanapakpawin et al. (2006) also found this same agreement of runoff peak timing and underestimation of annual flow volume when running DHSVM for a catchment in Northwestern Thailand. This is likely caused by misrepresentation of soil depth, infiltration (hydraulic conductivity), structural features, macropores, and other factors impacting base flow (Zecharias and Brutsaert, 1988) resulting from model parameterization. However, a newer version of DHSVM (version 3.0) than what was used in this study (version 2.0) is available that handles soil structure slightly different that may alleviate the errors with base flow underestimation (Doten et al., 2006).

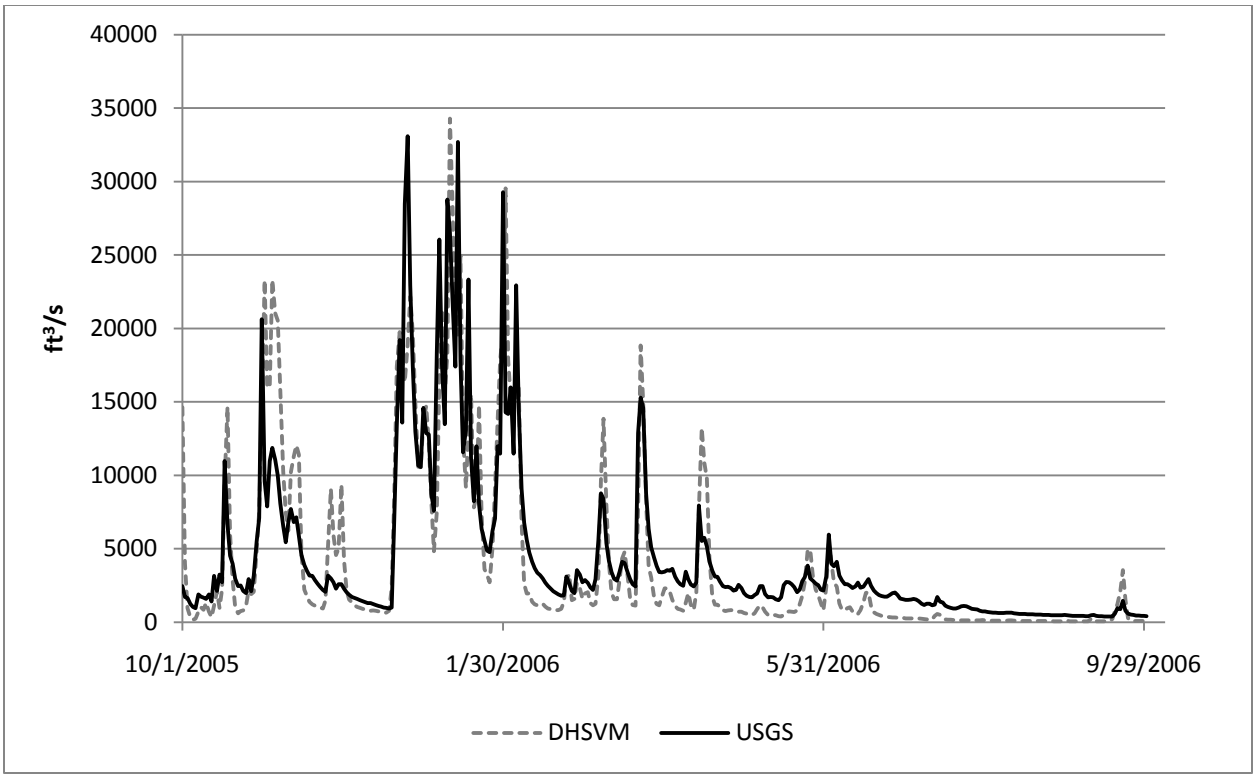

Figure 5 – Discharge results (ft^3/s) of DHSVM run with precipitation data uncorrected for PRISM underestimation compared to observed USGS stream gauge data at station 12040500.

Table 2 – Observed USGS stream gauge, calculated PRISM, and meteorological data depths in in/yr. Runoff coefficients represent dividing the observed runoff by the calculated PRISM precipitation volumes.

	in/yr			**Runoff Coefficient**	
Year	*USGS*	*PRISM*	*Met Data*	*PRISM*	*Met Data*
1996	128.70	154.85	152.83	0.83	0.84
1997	202.85	178.95	177.28	1.13	1.14
1998	148.47	151.35	157.85	0.98	0.94
1999	185.31	172.57	178.23	1.07	1.04
2000	99.81	106.40	103.80	0.94	0.96
2001	128.35	140.33	132.02	0.91	0.97
2002	134.16	126.08	121.35	1.06	1.11
2003	150.82	151.20	147.37	1.00	1.02
2004	110.68	118.84	115.66	0.93	0.96
2005	114.30	123.18	124.87	0.93	0.92
2006	150.09	148.27	156.82	1.01	0.96
			Average =	**0.98**	**0.99**

3.2 TEMPORAL EFFECTS

A total of 31 different precipitation cases were analyzed corresponding to 1 base case, 2 emission scenarios, 3 GCM projections, and 5 rainfall events. The base case is defined as the runoff resulting from running DHSVM with the unmodified precipitation data. Total annual runoff was found to vary across the different GCMs, emission scenarios, and rainfall events (figure 6, 7a-f). The largest annual runoff resulted from precipitation changes associated with the BCCR-BCM2.0 model under the A1B emission scenario applied to the maximum monthly 3 hour events. This case resulted in a runoff volume of 150 x 10^9 ft^3 (4.27 x 10^9 m^3) corresponding to an approximately 20% increase from the base case. The smallest runoff volume of 105 x 10^9 ft^3/s (2.97 x

10^9 m^3/s) resulted in a decrease of nearly 16% from the unadjusted meteorological data runoff, and corresponds to the GISS-ER model under the B2 scenario with precipitation changes applied over the entire month.

Comparing all the resulting annual runoff and percent difference from the unadjusted meteorological data (figure 6, table 3) it was found that the GISS-ER model resulted in the most variance across the different rainfall events. A difference of nearly 32 billion cubic feet in total annual runoff volume was found between the results of 3 hour and monthly storm events under the A1B emission scenario. This equates to an approximately 1000 ft^3/s change in average annual flow, which is nearly 25% of the observed current average annual runoff for the basin. In contrast, the BCCR-BCM2.0 model changes resulted in very little variance of annual runoff across the different rainfall events. The largest difference exhibited for the BCCR-BCM2.0 model runs existed between the 3 hour and monthly storm events under the A1B emission scenario. These scenarios produced a difference of 0.44 billion cubic feet (12.5 million m^3) of total annual runoff, which equates to approximately a difference of 14 ft^3/s (0.4 m^3/s) change in average annual flow. The CCMA-31 model projections resulted in slightly more variance across the different storm events in total annual runoff volume as compared to BCCR-BCM2.0 but not as significant as the variance exhibited by the GISS-ER model projections. One interesting aspect of the results of total annual runoff volume for the storm events under the CCMA-31 model projections is that the monthly events did not result in the lowest runoff volume as occurred with the other two models. Instead, the 2 day and single day events resulted in the least amount of total annual runoff across the different storm events for the CCMA-31 model respectively for the A1B and B2 emission

scenarios. Under the A1B emission scenario, the difference in annual runoff volume between the 2 day and 3 hour events was approximately 3.6 billion cubic feet (0.10 billion m^3), or 113 ft^3/s (3.2 m^3/s) average annual runoff change.

(a)

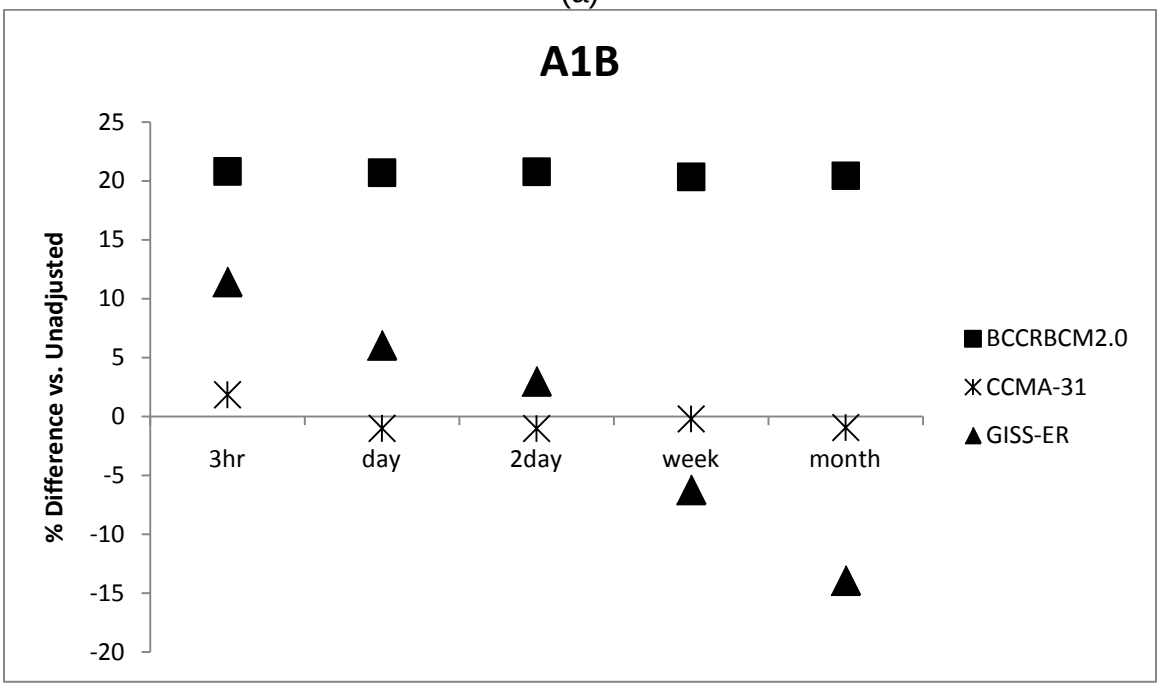

(b)

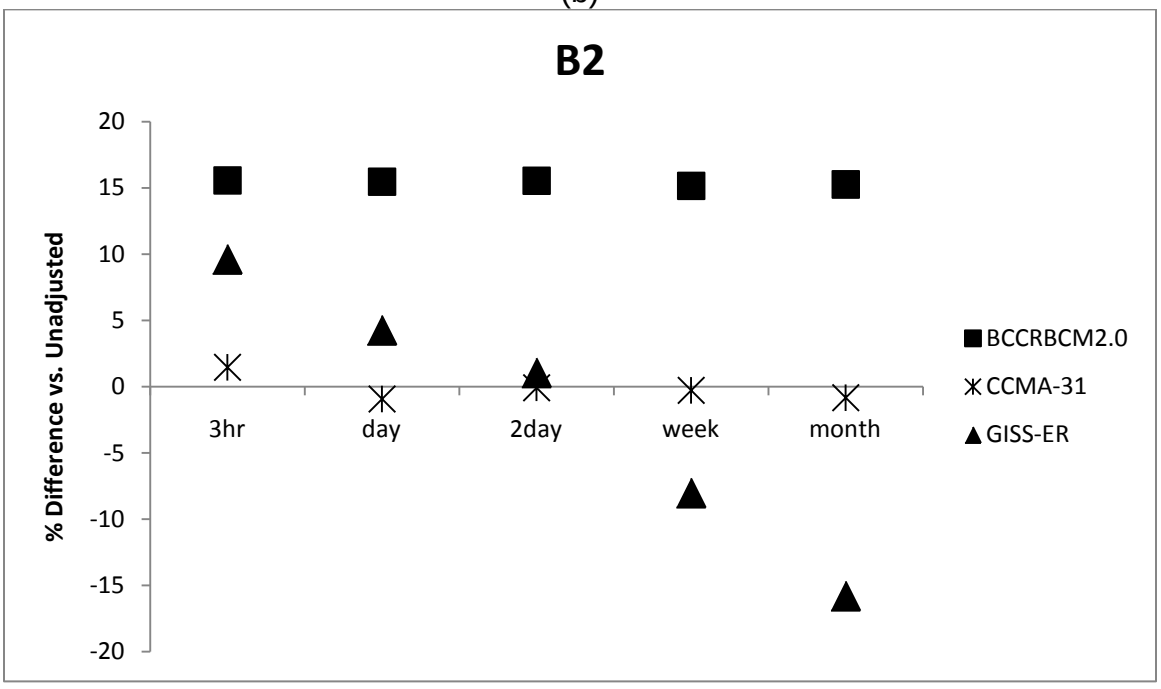

Figure 6 – Percent difference of annual runoff volume results from the unadjusted meteorological data for the 3 different GCMs for emission scenarios (a) A1B and (b) B2.

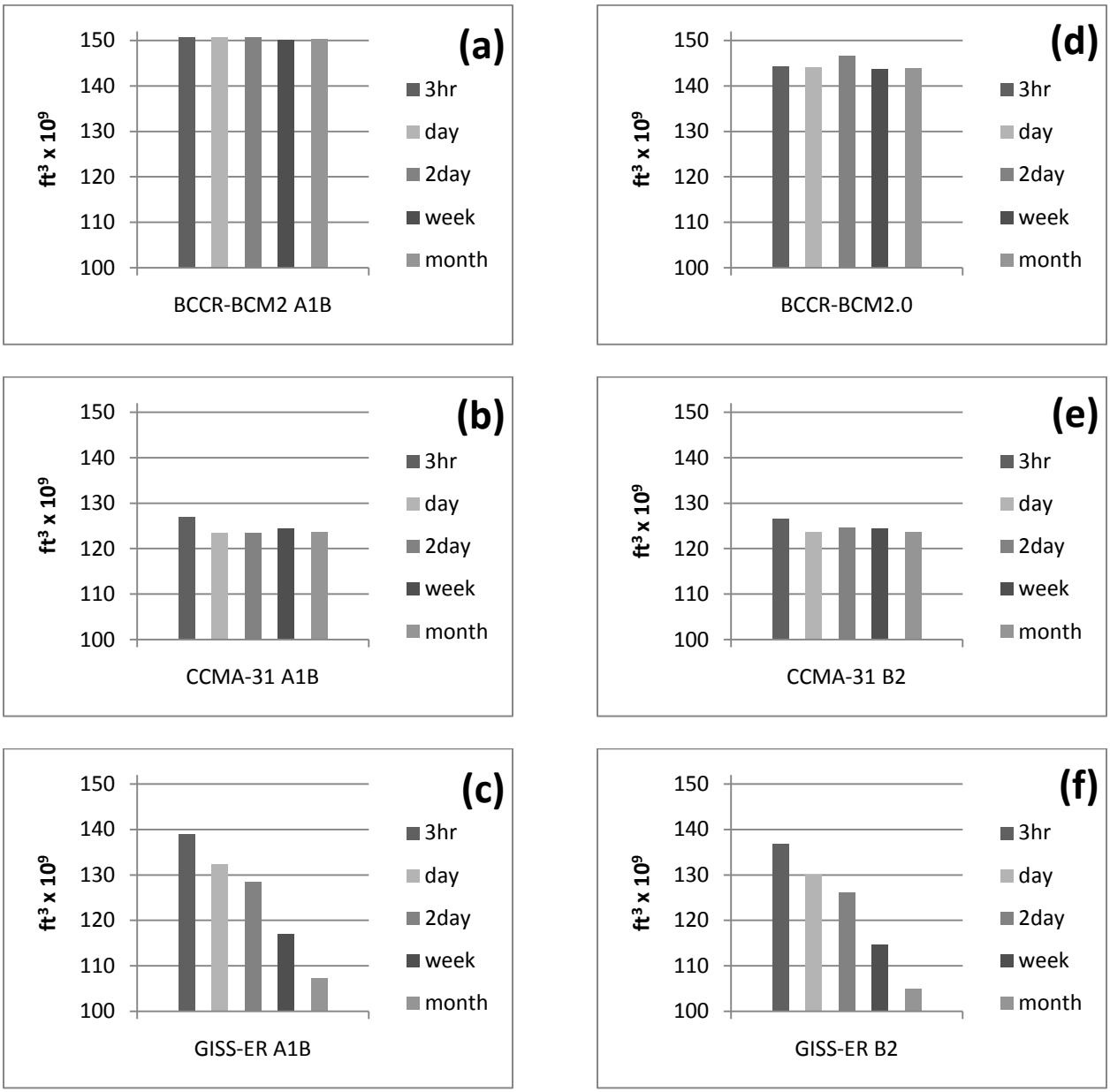

Figure 7 – Annual runoff volume (ft^3 x 10^9) resulting from applying projected precipitation changes to the 5 different rainfall events for (a) model BCCR-BCM2.0 emission scenario A1B, (b) model CCMA-31 emission scenario A1B, (c) model GISS-ER emission scenario A1B, (d) model BCCR-BCM2.0 emission scenario B2, (e) model CCMA-31 emission scenario B2, and (f) model GISS-ER emission scenario B2.

Time series plots comparing runoff results for the day, week, and month rainfall events were also made of the 3 different GCMs under the two emission scenarios (figure 8a-f). The reason for these plots was to compare the runoff timing and magnitude of peak events. The runoff timing of peak events and base flows compared well across all cases, but the magnitude of peak events was found to vary significantly. The largest variance in peak event magnitude occurred during winter or wet season months. Most notably, peak event magnitudes for the BCCR-BCM2.0 model were found to increase by more than 40,000 ft^3/s (1,133 m^3/s) in January for 3 hr duration changes as opposed to monthly changes (figure 9). Other notable months that exhibited large differences (greater than 10,000 ft^3/s (283 m^3/s)) in peak event magnitudes for the BCCR-BCM2.0 model were October, December, and March (figure 9a). The GISS-ER model also resulted in large differences in peak event runoff magnitude between the 3 hour and month long storm events (figure 9b). The largest differences were exhibited in the month of November, with a difference of up to 19,000 ft^3/s (538 m^3/s). Other months exhibiting differences between the 3 hour and month long storm event results of more than 10,000 ft^3/s (283 m^3/s) for the GISS-ER model include December, January, and March. Under the CCMA-31 model no peak runoff event magnitudes were found to differ by more than 9,000 ft^3/s (256 m^3/s) between the 3 hour and month long storm events, and the largest differences were displayed in November.

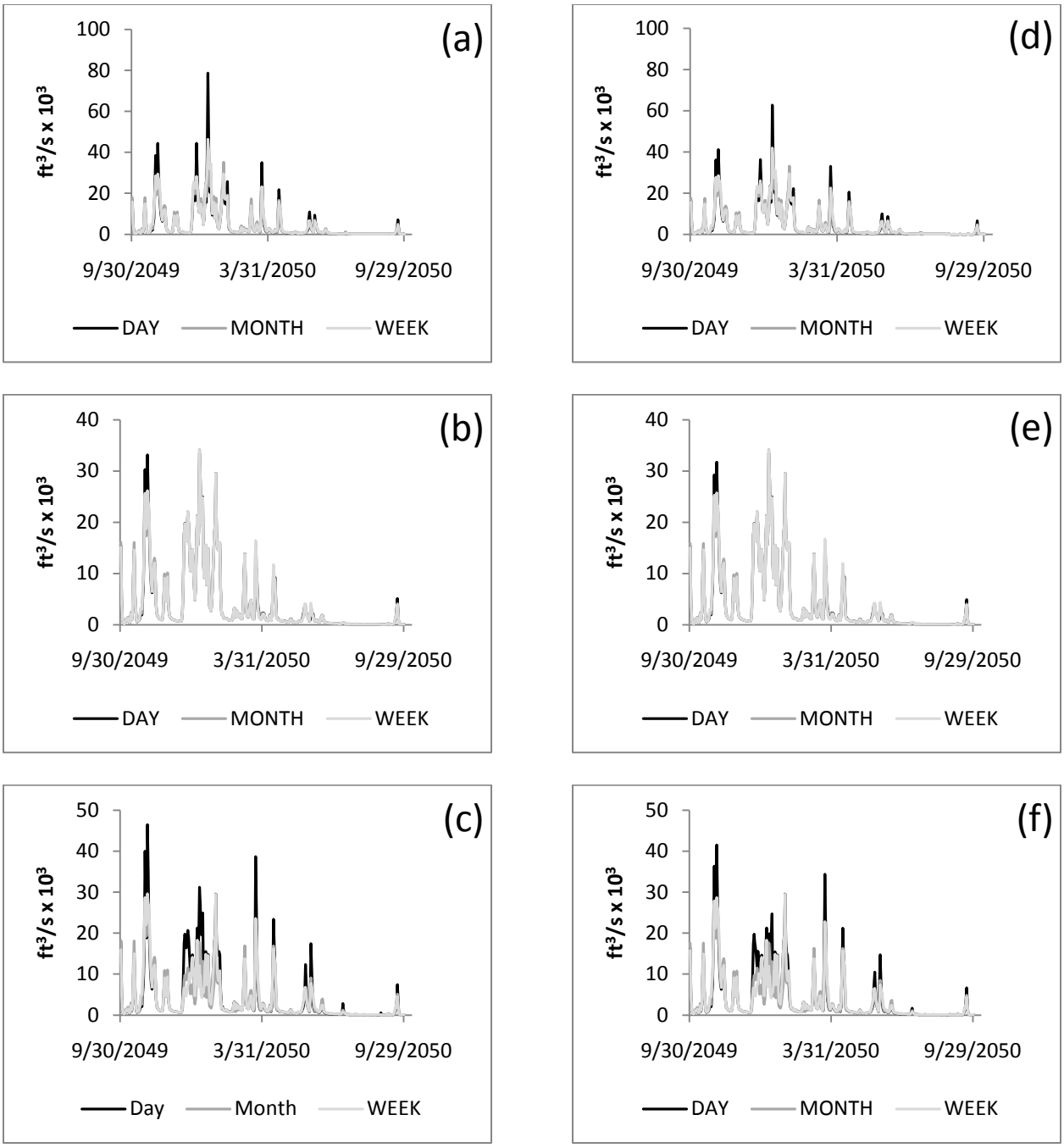

Figure 8 – Time series runoff results (ft^3/s) comparison for 1 day, 7 day, and month rainfall events for (a) model BCCR-BCM2.0 emission scenario A1B, (b) model CCMA-31 emission scenario A1B, (c) model GISS-ER emission scenario A1B, (d) model

BCCR-BCM2.0 emission scenario B2, (e) model CCMA-31 emission scenario B2, and (f) model GISS-ER emission scenario B2.

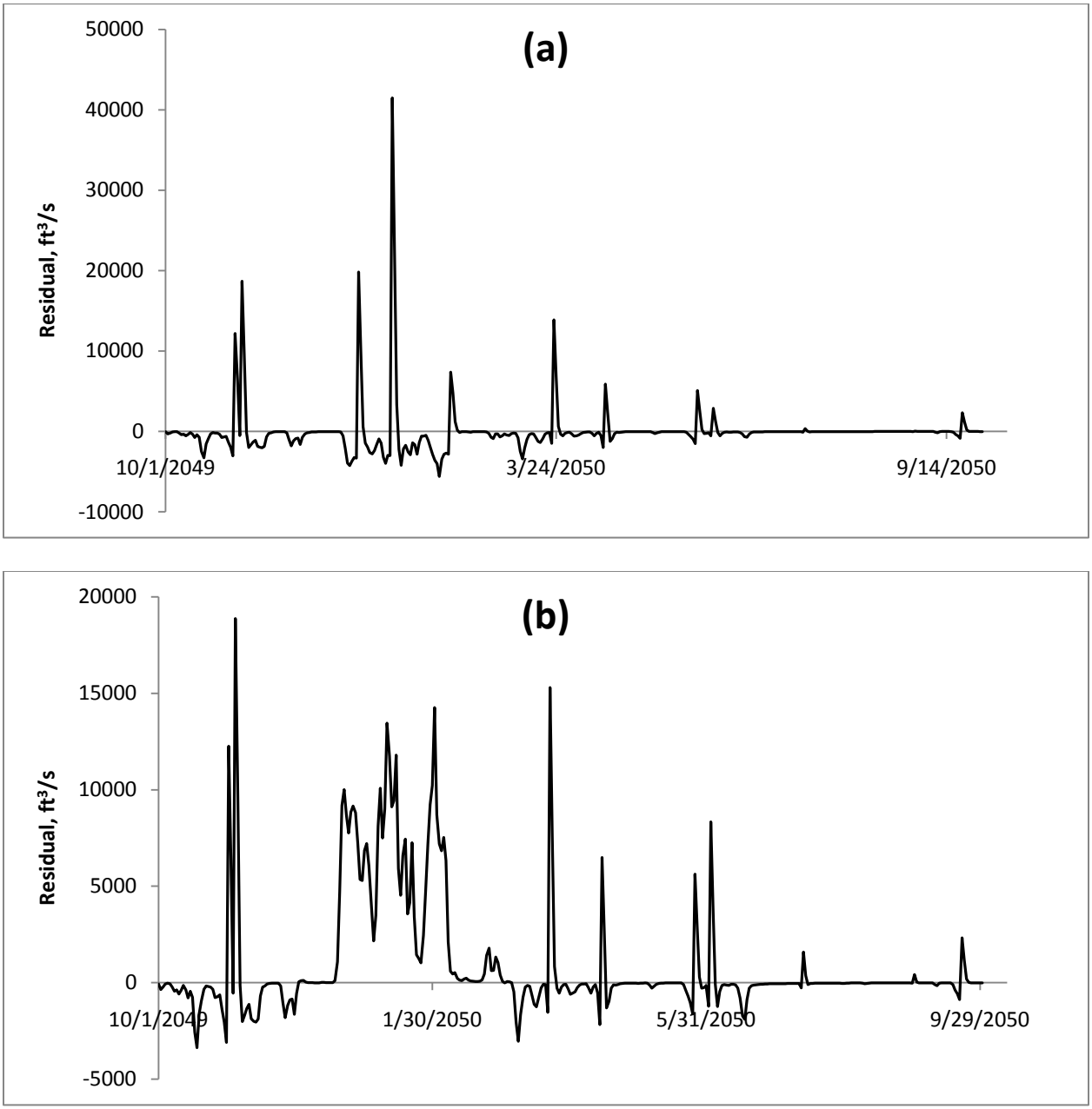

Figure 9 – residual plot between runoff results of the 3 hour storm event minus the runoff results of the month long storm event for the (a) BCCR-BCM2.0 model, A1B emission scenario, and (b) GISS-ER model, A1B emission scenario.

4.0 CONCLUSION

Careful examination and evaluation of interpolated precipitation forcings should be conducted when using DHSVM to model basin hydrology. From the results shown for the PRISM and meteorological data (Deems and Hamlet, 2010) evaluation it is concluded that as little as 61% of the actual precipitation may be represented by these two datasets, assuming a true runoff coefficient of 0.60. However, without physical observations of the basin hydrology it is difficult to determine the magnitude of underestimation. DHSVM underestimates the resulting runoff by approximately 9% for runs conducted using the meteorological data discussed. The runoff timing and magnitude of high flow events compare well between the DHSVM results and observed USGS stream gauge data. However, there exist underestimation errors during low flow conditions.

More work should be undertaken investigating the parameterization of DHSVM soil properties in an attempt to more accurately represent the true physical characteristics of the OESF and outflow processes. Specifically for the Queets watershed and OESF region, more data needs to be acquired concerning the actual soil properties. As this data is acquired it can be incorporated into the DHSVM model so a more accurate representation of the hydrology of the Queets watershed can be obtained. When using spatially interpolated rainfall data careful consideration of its representation of the actual precipitation should be made before calibrating the DHSVM model. Precipitation data that correlates well with the actual precipitation processes

allows for objective evaluation of other parameters influencing the hydrology in DHSVM such as soil properties.

The intensity and duration of precipitation changes projected for global climate change affect the runoff differently for different GCMs and emission scenarios. Depending on which future climate scenario actually occurs it is necessary to improve temporal downscaling techniques in order to correctly estimate the timing of future precipitation changes and ultimately aid in landslide prediction. From the results shown, temporal precipitation predictions at the daily time scale are necessary when estimating the magnitude of peak events under the BCCR-BCM2.0 and GISS-ER models (figure 9,10), and for predicting total annual runoff under the GISS-ER model (figure 6a,b). This can be broadened to include all GCM projections that predict large changes in winter precipitation for the OESF.

The high amount of variance in total annual runoff resulting from the GISS-ER model is thought to be a direct result of the large negative change in winter precipitation predicted. The annual runoff volume results (figure 6a,b;7c,f) show that reducing precipitation of one or even a couple of days will have a reduced effect on runoff then if reduced precipitation is experienced over longer time spans. This is because a longer time period of decreased precipitation has a stronger affect on the soil moisture and ultimately the runoff (Beljaars et al., 1996). That is why it can be observed that a steady decrease in runoff exists as the length of the storm event increases. This result is expected for catchments receiving high amounts of annual precipitation and/or containing high levels of soil moisture. Under this or a similar scenario it would be vitally important to have accurate high resolution temporal scale meteorological data

when making hazard predictions because of the range in runoff volume resulting from differences in storm event duration and intensity.

In contrast, varying storm event duration had little effect on annual runoff volumes for the region under scenarios of increased precipitation. This can be observed by looking at the annual runoff volume results of the BCCR-BCM2.0 model (figure 7a,d). This is thought to be a result of saturated soil conditions during the wet winter season, meaning that additional precipitation occurring on saturated soil will all result in runoff under any storm duration. However, the magnitudes of peak runoff events are much higher for the shorter duration storms because of differences in travel times required for the total projected change in precipitation to reach the basin outlet. For example, if changes in precipitation occur over a 3 hour time increment the total change in precipitation resulting in runoff will all reach the basin outlet within approximately a 3 hour interval. In contrast, month long precipitation changes will take the entire month to reach the outlet. Because intensity and duration are inversely proportional to one another under a constant change in runoff/precipitation, the runoff intensity would be much higher for a short duration event as in exhibited for the results shown in figure 8a,d.

Additional work should be conducted in regards to determining the GCM that best represents the physical processes and characteristics of the OESF so a better estimate of the precipitation change expected to occur can be made. This information can then be used in conjunction with the results given in this study to determine the accuracy and resolution required of the precipitation data to make confident runoff and hazard analysis predictions. In addition, quantifying the relationship between runoff and

landslide occurrences would allow hazard assessment predictions to be made based from runoff results. Another aspect that should be investigated concerns the spatial distribution of GCM projected precipitation change. Instead of applying projected precipitation changes uniformly across all grid cells in the spatial extent, it should be noted that higher elevation grid cells will likely experience more days of precipitation than lower elevation grid cells. This relationship should be investigated to determine the impact it has on runoff.

The storm duration under which GCM projected precipitation changes occur may have a large impact on runoff and hazard predictions in the OESF depending on the magnitude of change. If large changes in precipitation are expected, it is important to gain confidence in downscaling techniques in order to effectively project climate change situations. That way, accurate estimates of runoff volumes and peak event magnitudes can be predicted using dynamic modeling techniques.

REFERENCES

Adam, J. C., D. P. Lettenmaier. (2006). Adjustment of global gridded precipitation for systematic bias. Journal of Geophysical Research, Vol. 108, 4257, doi:10.1029/2002JD002499.

Anders, A. M., G. H. Roe, D. R. Durran and J. R. Minder. (2006). Small-scale spatial gradients in climatological precipitation on the Olympic Peninsula. Journal of Hydrometeorology, Vol. 32, pp 408-450.

Beljaars, A. C. M., P. Viterbo, M. J. Miller. (1996). The anomalous rainfall over the United States during July 1993: sensitivity to land surface parameterization and soil moisture anomalies. Monthly Weather Review, Vol. 124, pp 362-383.

Bevin, K. and A. Binley. (1992). The future of distributed models – model calibration and prediction. Hydrological Processes, Vol. 6(3), pp 279-298.

Bloschl, G. and M. Sivapalan. (1995). Scale issues in hydrologic modeling – a review. Hydrological Processes, Vol. 9(3-4), pp 251-290.

Boorman, D. B., J. M. Hollis, A. Lilly. (1995). Hydrology of soil types: a hydrologically based classification of the soils of the United Kingdom. IAHS Report, No. 126, pp 137.

Bowling, L. C., P. Storck and D. P. Lettenmaier. (2000). Hydrologic effects of logging in western Washington, United States. Water Resources Research, Vol. 36, pp 3223-3240.

Bowling, L. C., D. P. Lettenmaier. (2001). The Effects of Forest Roads and Harvest on Catchment Hydrology in a Mountainous Maritime Environment. Water Science and Application, Vol. 2, pp 145-164.

Brown, D.P. and A.C. Comrie. (2002). Spatial modeling of winter temperature and precipitation in Arizona and New Mexico, USA. Climate Research, Vol 22, pp 115-128.

Chow, V. T., D. R. Maidment, L. W. Mays. (1988). Applied Hydrology. Singapore. McGraw-Hill Book Company.

Chiew, F. H. S., T. I. Harrold, L. Siriwardena, R. N. Jones, R. Srikanthan. (2003). Simulation of climate change impact on runoff using rainfall scenarios that consider daily patterns of change from GCMs. MODSIM.

Colle, B. A., K. J. Westrick and C. F. Mass. (1999). Evaluation of MM5 and Eta-10 precipitation forecasts over the Pacific Northwest during the cool season. Weather and Forecasting, Vol. 14, pp 137-154.

Cuo, L., T. W. Giambelluca, A. D. Ziegler, M. A. Nullet. (2006). Use of the distributed hydrology soil vegetation model to study road effects on hydrological processes in Pang Khum Experimental Watershed, northern Thailand. Forest Ecology and Management, Vol. 224, pp 81-94.

Dai, F.C. and C.F. Lee. (2001). Frequency-volume relation and prediction of rainfall-induced landslides. Engineering Geology, Vol. 59, pp 253-266.

Daly, C., R. P. Neilson and D. L. Phillips. (1994). A statistical-topographic model for mapping climatological precipitation over mountainous terrain. Journal of Applied Meteorology, Vol. 33, pp 140-158.

Daly, C., G.H. Taylor, W.P. Gibson, T.W. Parzybok, G.L. Johnson and P.A. Pasteris. (2000). High-quality spatial climate data sets for the United States and beyond. Transactions of the ASAE, Vol. 43, pp 1957-1962.

Daly, C., W.P. Gibson, G.H. Taylor, G.L. Johnson and P. Pasteris. (2002). A knowledge-based approach to the statistical mapping of climate. Climate Research, Vol. 22, pp 99-113.

Deems, J., and A.F. Hamlet. (2010). Historical Meteorological Driving Data Set. (in review).

Diffenbaugh, N. S., J. S. Pal, R. J. Trapp and F. Giorgi. (2005). Fine-scale processes regulate the response of extreme events to global climate change. PNAS, Vol. 102, pp 15774-15778.

Doten, C. O., L. C. Bowling, J. S. Lanini, E. P. Maurer, and D. P. Lettenmaier. (2006), A spatially distributed model for the dynamic prediction of sediment erosion and transport in mountainous forested watersheds, Water Resour. Res., 42, W04417, doi:10.1029/2004WR003829.

D. Sutherland. (2006). Policy for sustainable forests. Washington State Dept. of Natural Resources.

Elsner, M. M., L. Cuo, N. Voisin, A. F. Hamlet, J. S. Deems, D. P. Lettenmaier, K. E. B. Mickelson, and S. Y. Lee. (2010). Implications of 21st century climate change for the hydrology of Washington State. Climate Change (in review).

Fu, G., M.E. Barber, and S. Chen. (2009). Hydro-climatic variability and trends in Washington State for the last 50 years. Hydrological Processes, Early View, On-line.

Guan, H., J.L. Wilson, and O. Makhnin. (2005). Geostatistical mapping of mountain precipitation incorporating autosearched effects of terrain and climatic characteristics. Journal of Hydrometeorology, Vol 6, pp 1018-1031.

Guzzetti, F., S. Peruccacci, M. Rossi, C. P. Stark. (2008). The rainfall intensity-duration control of shallow landslides and debris flows: an update. Landslides, Vol. 3, pp 3-17.

Hamlet, A. F., D. P. Lettenmaier. (2005). Production of temporally consistent gridded precipitation and temperature fields for the continental United States. Journal of Hydrometeorology, Vol. 6, pp 330-336.

Heany, J.P., W.C. Huber, and S.J. Nix. (1976). Storm water management model: level I – preliminary screening procedures. US EPA Report 66/2-76-275, Cincinnati, OH.

Horner, R. R. (1985). *Highway Runoff Water Quality Research Implementation Manual.* Seattle, WA: Washington State Dept. of Transportation.

Houghton, J.G. (1979). A model for orographic precipitation in the north-central Great Basin. Monthly Weather Review, Vol. 107, pp 1462-1475.

Hultstrand, D., T. Parzybok, E. Tomlinson, B. Kappal. (2008). Advanced spatial and temporal rainfall analyses for use in watershed models. Third Interagency Conference on Research in the Watersheds, pp 245-250.

Intergovernmental Panal on Climate Change. (2000) Summary for Policymakers: Emissions Scenarios. A special report of IPCC Working Group III.

Iverson, R. (2000). Landslide triggering by rain infiltration. Water Resources Research, Vol. 36, pp 1897-1910.

Jakeman, A.J. and G.M. Hornberger. (1993). How much complexity is warranted in rainfall-runoff model. Water Resources Research, Vol. 29(8), pp 2637-2649.

Kadiglu, M. and Z. Sen. (1995). Power-law relationship in describing temporal and spatial precipitation pattern in Turkey. Theoretical and Applied Climatology, Vol 59(1-2), pp 93-106.

Kalnay, E., M. Kanamitsu, R. Kistler, W. Collins, D. Deaven, L. Gandin, M. Iredell, S. Saha, G. White, J. Woollen, Y. Zhu, A. Leetmaa, R. Reynolds, M. Chelliah, W. Ebisuzaki, W.Higgins, J. Janowiak, K. C. Mo, C. Ropelewski, and J. Wang. (1996). The NCEP/NCAR 40-Year Reanalysis Project. Buletin of American Meteorological Society, Vol. 77, pp 437-471.

Katimon, A. and A.K.A. Wahab. (2003). Hydrologic characteristics of a drained tropical peat catchement: runoff coefficients, water table and flow duration curves. Jurnal Teknologi, Vol.38, pp 39-54.

Katz, R. W., B. G. Brown. (1992) Extreme events in a changing climate: Variability is more important than averages. Earth and Environmental Science, Vol. 21, pp 289-302.

Kidd, C., D. R. Kniveton, M. C. Todd, T. J. Bellerby. (2003). Satellite rainfall estimation using combined passive microwave and infrared algorithms. Journal of Hydrometeorology, Vol. 4, pp 1088-1104.

Lamarche, J. and D.P. Lettenmaier. (1998). Forest road effects on flood flows in the Deschutes river basin, Washington. Water Resource Series, Technical Report, Department of Civil Engineering, University of Washington.

Leung, L. R. and M. S. Wigmosta. (1999). Potential climate change impacts on mountain watersheds in the Pacific Northwest. JAWRA, Vol. 35, pp 1463-1471.

Marquinez, J., J. Lastra, and P. Garcia. (2003). Estimation models for precipitation in mountainous regions: the use of GIS and multivariate analysis. Journal of Hydrology, Vol. 270(1-2), pp 1-11.

Miles, E. L., A. K. Snover, A. F. Hamlet, B. Callahan and D. Fluharty. (2000). Pacific Northwest regional assessment: the impacts of climate variability and climate change on the water resources of the Columbia River Basin. Journal of the American Water Resources Association, Vol. 36, pp 399-420.

Minder, J. R., D. R. Durran, G. H. Roe, and A. M. Anders. (2008). The climatology of small-scale orographic precipitation over. Quarterly Journal of the Royal Meteorological Society, Vol. 134, pp 817-839.

Moore, R.D. and S.M. Wondzell. (2005). Physical hydrology and the effects of forest harvesting in the Pacific Northwest: A review. Journal of the American Water Resources Association, Vol. 41(4), pp 763-784.

Nijssen, B. N., D. P. Lettenmaier, X. Liang, S. W. Wetzel, E. F. Wood. (1997). Streamflow simulation for continental-scale river basins. Water Resource Research, Vol. 33, pp 711-724.

Pandit, A. and G. Gopalakrishman. (1996). Estimation of annual storm runoff coefficients by continous simulation, ASCE Journal of Irrigation and Drainage, Vol. 122(4), pp 211-220.

Pauleit, S., R. Ennos, Y. Golding. (2005). Modeling the environmental impacts of urban land use and land cover change-a study in Merseyside, UK. Landscape and Urban Planning, Vol. 71, pp 295-310.

Peck, E. L. and M. J. Brown. (1962). An Approach to the Development of Isohyetal Maps for Mountainous Areas. Geophysical Research, Vol. 67, pp 681-694.

Polluck, M. M., S. Baker, R. Bigley and W. Scarlet. Summer stream temperatures in the Olympic Experimental State Forests, Washington. Northwest Fisheries Science Center, Seattle, WA: Department of Natural Resources Habitat Conservation Plan Stream and Riparian Monitoring Program, 2004.

Rahardjo, H., X. W. Li, D. G. Toll and E.C. Leong. (2001). The effect of antecedent rainfall on slope stability. Geotechnical and Geological Engineering, Vol. 19, pp 1573-1529.

Roche, M. A. (1981). Watershed investigations for development of forest resources of the Amazon Region in French Guyana. Tropical Agriculture Hydrology, pp 75-82.

Schueler, T.R. (1987). Controlling urban runoff: a practical manual for planning and designing urban BMPs. Metropolitan Washington Council of Governments, Publ. No. 87703. Washington, DC.

Semenov, M. A., E. M. Barrow. (1997). Use of a stochastic weather generator in the development of climate change scenarios. Earth and Environmental Science, Vol. 35, pp 397-414.

Sen, Z. and Z. Habib. (2000). Spatial precipitation assessment with elevation by using point cumulative semivariogram technique. Water Resources Management, Vol 14(4), pp 311-325.

Serreze M.C., R.S. Pulwarty, M.P. Clark, R.L. Armstrong, and D.A. McGinnis. (1999). Characteristics of the western United States snowpack from snowpack telemetry (SNOTEL) data. Water Resour Res, Vol 35, pp 2145–2160.

Smith, R. B.. (1979). The influence of mountains on the atmosphere. Advances in Geophysics, Vol. 27, Academic Press, pp 87-230.

Stehlik, J. I., A. Bardossy. (2002). Multivariate stochastic downscaling model for generating daily precipitation series based on atmospheric circulation. Journal of Hydrology, Vol. 256, pp 120-141.

Storck, P., L. Bowling, P. Wetherbee, and D. Lettenmaier. (1995). Application of a GISbased distributed hydrology model for prediction of forest harvest effects on peak stream flow in the Pacific Northwest. Hydrological Processes, Vol. 12(6), pp 889-904.

Storck, P., D. P. Lettenmaier, B. A. Connelly and T. W. Cundy, (1995). Implications of forest practices on downstream flooding: Phase II Final Report, Washington Forest Protection Association, TFW-SH20-96-001.

Storck P, Bowling L, Wetherbee P, Lettenmaier D. (1998). Application of a GIS-based distributed hydrology model for prediction of forest harvest effects on peak stream flow in the Pacific Northwest. Hydrological Processes, Vol. 12, pp 889–904.

Terlien, M. T. J. (1998). The determination of statistical and deterministic hydrological landslide-triggering thresholds. Environmental Geology, Vol. 35, pp 124-130.

Thanapakpawin, P., J. Richey, D. Thomas, S. Rodda, B. Campbell, M. Logsdon. (2006). Effects of landuse change on the hydrologic regime of the Mae Chaem River basin, NW Thailand. Journal of Hydrology, Vol. 334, pp 215-230.

Thiessan, A. H. (1911). Climatological data for July, 1911. Monthly Weather Review, Vol. 39, pp 1082-1084.

Thornton, P. E., S. W. Running, M. A. White. (1997). Generating surfaces of daily meteorological variables over large regions of complex terrain. Journal of Hydrology, Vol. 190, pp 214-251.

Wigmosta, M. S., L. W. Vail, D. P. Lettenmaier. (1994). A distributed hydrology-vegetation model for complex terrain. Water Resources Research, Vol. 30, pp 1665-1679.

Wigmosta, M.S. and W.A. Perkins. (2001). Simulating the effects of forest roads on watershed hydrology, in Influence of Urban and Forest Land Use on the Hydrologic-Geomorphic Responses of Watersheds, M.S. Wigmosta and S.J. Burges, eds., AGU Water Science and Applications Series, 2, in press, 2001.

Wigmosta, M. S., B. Nijssen, and P. Storck. (2002). The distributed hydrology soil vegetation model. Mathematical Models of Small Watershed Hydrology Applications, edited by V. P. Singh and D. K. Frevert, pp. 7–42, Water Resource Publications, Highlands Ranch, Colorado.

Wiley, M. W. and R. N. Palmer. (2008). Estimating the impacts and uncertainty of climate change. Water Resources Planning and Management, Vol. 134, pp 239-246.

Xu, C-Y and S. Halldin. (1997). The effect of climate change on river flow and snow cover in the NOPEX area simulated by a simple water balance model. Nordic Hydrology, 28 (4/5), pp 273-282.

Yang, D. and T. Ohata. (2001). A bias-corrected Siberian regional precipitation climatology. Journal of Hydrometeorology, Vol. 2, pp 122-139.

Zecharias, Y.B. and W. Brutsaert. (1988). Recession characteristics of groundwater outflow and base flow from mountainous watersheds. Water Resour. Res., Vol. 24(10), pp 1651–1658.

Zezere, J. L., A. B. Ferreira, M. L. Rodrigues. (1999). Landslides in the North of Lisbon region (Portugal): conditioning and triggering factors. Physics and Chemistry of the Earth, Part A: Solid Earth and Geodesy, Vol. 24, pp 925-934.

Zhang, X. and R. Srinivasan. (2009). GIS-based spatial precipitation estimation: a comparison of geostatistical approaches. Journal of the American Water Resources Association, Vol 45(4), pp 894-906.

Zimmermann, N.E. and D.W. Roberts. (2001). Final Report of the MLP climate and biophysical mapping project. MLP climate mapping project. Swiss Federal Research Institute WSL, Birmensdorf, Switzerland.